Plasma Chem Plasma Process (2016) 36:45–72
DOI 10.1007/s11090-015-9652-7

REVIEW ARTICLE

Plasma Catalysis for Environmental Treatment and Energy Applications

Hyun-Ha Kim[1] · Yoshiyuki Teramoto[1] · Atsushi Ogata[1] · Hideyuki Takagi[1] · Tetsuya Nanba[2]

Received: 4 July 2015 / Accepted: 20 August 2015 / Published online: 16 October 2015

Abstract The current status of plasma-catalysis research and the associated possible applications are outlined. A basic explanation of plasma chemistry is given, which is then used as a foundation to indicate the research vector for the ongoing development of various applications. As an example of an environmental application, volatile organic compound decomposition using plasma-catalysis is discussed in depth, from the fundamental concept to the current industrial application status. As a potential application of plasma-catalysis towards the realization of a future "hydrogen society", ammonia synthesis is discussed in terms of current social attitudes and regulations, along with historical developments. Additionally, up-to-date information on the fundamentals of the nonthermal plasma interaction with a catalyst is provided.

Keywords Nonthermal Plasma · Catalyst · Plasma-catalysis · VOC decomposition · NH_3 synthesis

Introduction

Nonthermal plasma (NTP) can induce various chemical reactions at both atmospheric pressure and normal ambient temperature, and the formation of highly reactive short-lived species and the subsequent chemical reactions are intrinsic aspects of plasma chemistry. The chemical potential of NTP has been studied with regard to various applications, such as volatile organic compound (VOC) decomposition, NOx and SOx removal, ozone

✉ Hyun-Ha Kim
hyun-ha.kim@aist.go.jp

[1] National Institute of Advanced Industrial Science and Technology (AIST), 16-1 Onogawa, Tsukuba, Ibaraki 305-8569, Japan

[2] Fukushima Renewable Energy Institute (FREA), National Institute of Advanced Industrial Science and Technology (AIST), 2-2-9 Machiikedai, Koriyama, Fukushima 963-0298, Japan

generation, surface treatments, hydrogen (H_2) formation, fuel reforming, and biomedical use. In particular, the application of electrical discharge plasmas in environmental treatment techniques became a prominent topic of research in the mid-1980s and 1990s [1–4]. As regards the social context motivating this interest, various environmental regulations were introduced or reinforced worldwide during that period. The Clean Air Act amendment in 1990 (USA) aimed to curb three major environmental problems: acid rain, urban air pollutants, and air toxics [5]. This amendment included 189 toxic air pollutants of which emissions must be reduced. Similar stringent regulations were introduced in other countries: the Chemical Release Inventory (CRI, UK 1991), the European Polluting Emission Register (EPER, EU 1996), and the Pollutant Release and Transfer Register (PRTR, 1999 Japan). The first international conference focusing on NTP technologies for environmental treatment applications was held at Cambridge, and collections of the contributed papers were published in two books edited by the late Bernie Penetrante [6, 7]. In the1990s, NTP was widely studied for application in the removal of various pollutants such as NOx [8–10], SOx [2, 11–14], odor [15] and VOCs [4, 16–24], under moderate reaction conditions (i.e., ambient temperature and atmospheric pressure). At that time, many researchers believed that plasma could achieve the required reactions without catalysts, and this was even considered to be one of the important advantages of NTP [25]. However, as a wide range of experimental data was compiled during the 1990s, several limitations that arise when NTP is used alone were identified, such as large energy consumption, and formation of unwanted byproducts. As plasma is essentially an electrically transformed material, energy consumption is a priority in any kind of plasma chemistry. Thus, as a reasonable approach to overcoming these problems, the combination of NTP and other techniques has been an active area of research since 2000. Many different techniques as NTP counterparts have been considered including catalysts, adsorption, wet-scrubbing [26–30], bio-filtration [31], and filter [32]; these combinations have been proven to be efficient. Figure 1 briefly summarizes the application areas of plasma-catalysis. The environmental treatment applications include VOC and odor removal [33–36], NOx reduction [37–40], and water treatment [41–43]. As regards energy applications, the use of plasma-catalysis for dry reforming, syngas production, hydrogen production, methanation, and ammonia (NH_3) synthesis has been studied. Catalyst preparation using plasma is beyond the scope of this review [44–46]; however this topic may be of importance in

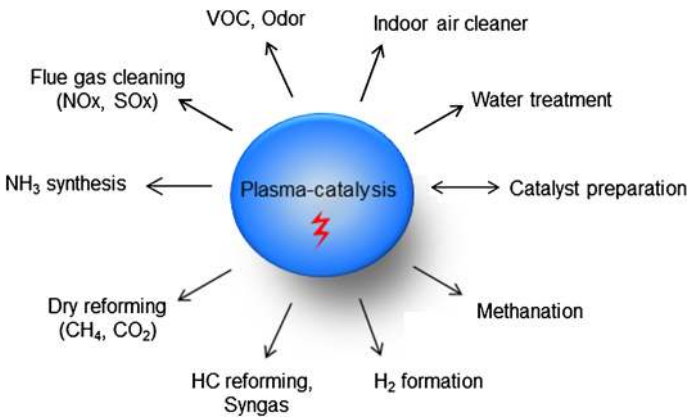

Fig. 1 Applications of plasma-catalysis

relation to plasma-catalysis, because changes in catalyst properties (morphology, dispersion, redox, etc.) can also occur during the reactions.

Research into both plasma and catalysts has a centuries-old history, from early investigations to industrial applications. The complementary combination of NTP and catalysts offers various advantages in terms of energy efficiency, product selectivity, and carbon balance. Understanding the physical interaction between NTP and a catalyst is important for further optimization of a given system. However, this field is still in the early research stages and fundamental information on the interaction of NTP with a catalyst is still lacking; thus, further study is required. In this review, recent progress concerning elucidation of the mechanism underlying plasma-catalysis will be discussed. VOC decomposition will be discussed as an example of an environmental treatment application and NH_3 synthesis will be reviewed as an energy-related issue. Some relevant open questions on the elementary steps of plasma catalysis, which may yet be answered, will also be addressed. Note that, for convenience, the conventional catalytic reactions under the effects of heating will be hereinafter referred to as "thermal catalysis".

Early Studies of Catalytic Effects in Electrical Discharges

Catalytic Actions in the Corona Electrode

Table 1 summarizes several examples of early studies of the catalytic effects confirmed in plasma chemical reactions. Selected studies from this table are discussed below, along with additional prominent reports. The use of silent discharge plasma for the removal of toxic gas and carbon monoxide (CO) was examined during World War I, but was found to be less effective for practical use. Ray and Anderegg tested CO oxidation using ozone (O_3)-assisted catalytic oxidation (i.e., a two-stage process) in the1920s [47]. They found that lead (Pb), lead oxide, and manganese dioxide (MnO_2) coated on glass wool can completely decompose O_3, but this does not apply to CO oxidation. However, silver (Ag) was found to be an active catalyst for CO oxidation with O_3. This study also identified the positive effect of moisture on CO oxidation. Another example of a catalytic effect is the dependence of O_3 formation on the electrode material in a corona discharge; this was also observed in the 1920s [48]. Further, it was noted that filling a reactor with glass wool increases the yield of active hydrogen [49], which may be due to the resultant uniform plasma [50]. Newsome tested O_3 decomposition (2 % O_3 in O_2) using a wire-to-cylinder reactor, and found that the decomposition increases based on the electrode material used, in the order: copper (Cu) > gold (Au > Ag > aluminium (Al) [51]. He also mentioned the aging effect, where the O_3 concentration increases with time, even under fixed conditions. In the case of Au, the decomposition decreases as its surface is oxidized through the formation of a thin film oxide. Boelter and Davidson [52] reported O_3 formation suppression in accordance with electrode material type in a two-stage wire-plate indoor air cleaner, which was operated with a positive polarity. They reported 30 and 50 % O_3 reduction with Cu and Ag wires, respectively, compared with standard tungsten (W) wire. Recently, Yehia and Mizuno reported the effect of electrode materials on O_3 formation in more detail. Six materials (Ag, W, Au, Cu, Ni, and Al) were examined, with Ag exhibiting the most prominent effect [53]. Furthermore, they also determined that the effect of Ag was more prominent in a positive corona in dry air than in a corona with negative polarity or in O_2. Maltsev and Belova reported that the packing of metallic gauze (Ag, CuO, Fe, or Pt) within a reactor enhanced

Table 1 Early landmark works of the plasma-catalysis (before 1990)

Year	Catalyst	Reactor	Pressure	Phenomena	Reference
1921	Ag, Mn, Pb	Two-stage	*	CO removal over ozone decomposition catalysts	B. Ray, *JACS* V43, 967–978
1923	Au, Pt	Single-stage	*	Dielectric packing decreases ozone formation	F. O. Anderegg, *Trans. Am. Electrochem Soc.* V44, 203–214
1926	Ag, Al, Au, Cu	Single-stage	*	The effect of electrode materials both on formation and decomposition of ozone	P. T. Newsome, *JACS*, V48, 2035–2045
1938	CuCl/coke breeze	Single-stage	*	Converting gaseous hydrocarbon into liquid hydrocarbon. The main role of the AC high frequency power ($\sim$20 kHz) was heating of the catalyst up to 800 °C.	E. C. Mills, US Patent 2139969
1941	14 materials	Single-stage	*	Gasoline production using combined process of electrical discharge and catalysts (summary of patents in 1920s–1930s)	C. L.Thomas, *Chem Rev*, V48, 1–70
1968	Pd, Ni, Au, Ag, Pd	Single-stage	6 Torr	Ammonia decomposition in glow discharge	E. A. Rubtsova, *Russ. J. Phys. Chem.*, V42, 536–539
1969	alumina	Single-stage	*	Alumina-packed DBD reactor for aromatic VOC removal	M. Kawahata, *Advances in Chem Series 80 (ACS)*, 316–321
1971	Pd, Pt	Single-stage	700 Torr	Ammonia synthesis from H_2-N_2 mixture in a barrier discharge. Metal wires wound on the inner electrode of the discharge tube.	E. N. Eremin, *Russ. J. Phys. Chem.*, V45(5), 635–638
1974	Activated carbon, alumina	Two-stage	*	Catalytic oxidation of hydrocarbons in the presence of ozone	K. Hauffe, *Chemie Ingenieur Technik*, V46, 1053
1976	8 materials	Single-stage	1 atm	NOx removal	Henis, US Patent 3983021
1978	Metallic gauze (Ag, CuO, Fe, Pt)	Single-stage	100 Torr	NO synthesis in a glow discharge	V.M. Belova, *Russ. J. Phys. Chem.*, V52, 968–970; 970–972
1986	MgO	Single-stage	10 Torr	Ammonia synthesis	K. Sugiyama, *Plasma Chem Plasma Proc*, V6, 179–193
1989	Silica (1.25–3.2 mm)	Single-stage	1 atm	Ozone formation increased by 1.4–1.6 times (based on ozone yield), g-O_3/kWh) with silica packing	K. Schmidt-Szalowski, *Plasma Chem Plasma Proc*, V9, 235–255
1989	Au	Single-stage	20 Torr	Enhanced conversion of CO to CO_2 in CO_2 laser coated with Au	J. A. Macken, *IEEE J Quantum Electro*., V25(7), 1695–1703
1989	NS	Multistage	*	De-odor reactor with three-stage plasma-catalyst bed ($BaTiO_3$-NOx CAT-O_3 CAT)	H. Yoshida, *J Electrostat Japan*, V13(5), 425–430

* Not specified

NO synthesis in a low-pressure glow discharge [54–58]. Chen et al. [59] investigated methyl chloride (CH_3Cl) removal using a metal (Fe, Pt or Au) coated electrode, which may function as a catalyst. From a practical perspective, metal nanoparticles supported on appropriate supports (TiO_2, γ-Al_2O_3, SiO_2, CeO_2, perovskite, zeolite) are more desirable catalysts than bulk materials (i.e., electrodes). For a given amount of active metals, the smaller the particle size, the larger the active sites on the surface; this is beneficial for the catalytic reaction.

Thomas et al [60] reported a brief summary of patents awarded in the 1920s–1930s for gasoline production involving the combination of electrical discharges and catalysts. The patent obtained by Henis for NOx removal was another important milestone in single-stage plasma-catalysis [61]. Even though Henis tested more than ten materials under various conditions (100 °C, space velocity up to 5000 h^{-1}, 50–86 watt input power, 1500–2000 ppm NO, gas composition primarily at 1 % O_2 and 10 % CO_2), the efficiency was low; this was because he focused on the direct decomposition of NOx rather than the use of a reducing agent. Nevertheless this phenomenal approach to plasma-catalysis is definitely worth noting, as it was devised in the 1970s, when the use of plasma in environmental treatment applications was not being considered.

Catalytic Effect on O_3 Generation

O_3 generation is the most thoroughly studied topic in plasma chemistry. However, controversy exists regarding the effect of the reactor packing material on the O_3 formation. For example, Schmidt-Szalowski et al. [62, 63] reported $\sim$1.6 fold enhanced O_3 formation obtained using silica packing materials in ozonizer in 1989. Morinaga and Suzuki also observed this effect in 1962 [64]. However, these papers did not consider the possible changes in energy input induced by the packing materials and comparisons based on energy efficiency were not given. It is worth noting that the plasma properties vary considerably under different dielectric barrier surface conditions. For example, Tanaka et al. [65] reported an increase of O_3 formation of approximately 20 % when chromium trioxide (CrO_3) was coated on a glass surface. They observed this phenomenon using a short-gap (<1 mm) O_2-fed ozonizer with a single barrier configuration (i.e., stainless steel-glass). The change in electrical discharge was also confirmed by comparing the V–Q Lissajous figures and was found to be due to electron emission from the surface when the gas was in negative potential. Recently, Toyofuku et al. [66] studied O_3 generation using six materials with different dielectric constants ε (glass: 7.5, Al_2O_3: 8.5, MgO: 30, TiO_2: 86, $SrTiO_3$: 332, $BaTiO_3$: 2900) and found that TiO_2 was most effective even though it is known as catalyst for O_3 decomposition. Further, Bo et al. [67] used multi-wall carbon nanotube (MWCNT) electrodes in an indoor air cleaner to minimize O_3 formation, and confirmed that the O_3 concentration was below the detection limit (0.5 ppb) for current densities up to 0.744 A/m^2. In contrast to the observed stability of the MWCNT electrode over 30 min, Liang et al. [68] reported gradual degradation of an MWCNT electrode with increasing numbers of discharge cycles. Yurevich et al. [69] indicated that the discharge mode in air-fed dielectric barrier discharge (DBD) varies with the surface conductivity of the dielectric material, while Osawa and Yoshioka reported glow-like homogeneous DBD in air at a frequency range of 32 Hz–1.1 kHz. They demonstrated that the electron emission from the alumina ceramic played an important role in this discharge mode [70]. Jodzis reported [71] that bell-shape O_3-poisoning does not appear in an air-fed ozonizer when silica beads (0.5–0.8 mm in diameter and 358 m^2/g surface area) are packed in the ozonizer. Several potential explanations were provided, such as NOx adsorption, reduced gas distance, gas

flow, and residence time. These results imply that packing materials can interact with plasma in different ways; therefore, we must examine these phenomena from a multidisciplinary perspective in order to determine a reasonable conclusion.

Raison d'Etre of Catalyst in Plasma Chemistry

Classification of Reactor Configurations

The plasma catalyst reactor combination types include single-, two- and multi-stage configurations, in accordance with the position and number of catalyst beds [72], as schematically illustrated in Fig. 2. In the single-stage plasma-catalysis system (a), the catalysts are located inside the plasma reactor. In contrast, catalysts are located downstream of the plasma reactor in the two-stage system (b). O_3-assisted catalysis is a two-stage process, where the role of the plasma is confined to the generation of O_3. Jia et al. [73] have reported a single-stage system for acetaldehyde removal, in that case, the catalysts were fluidized by the gas flow . The optimization of the catalyst and plasma can be

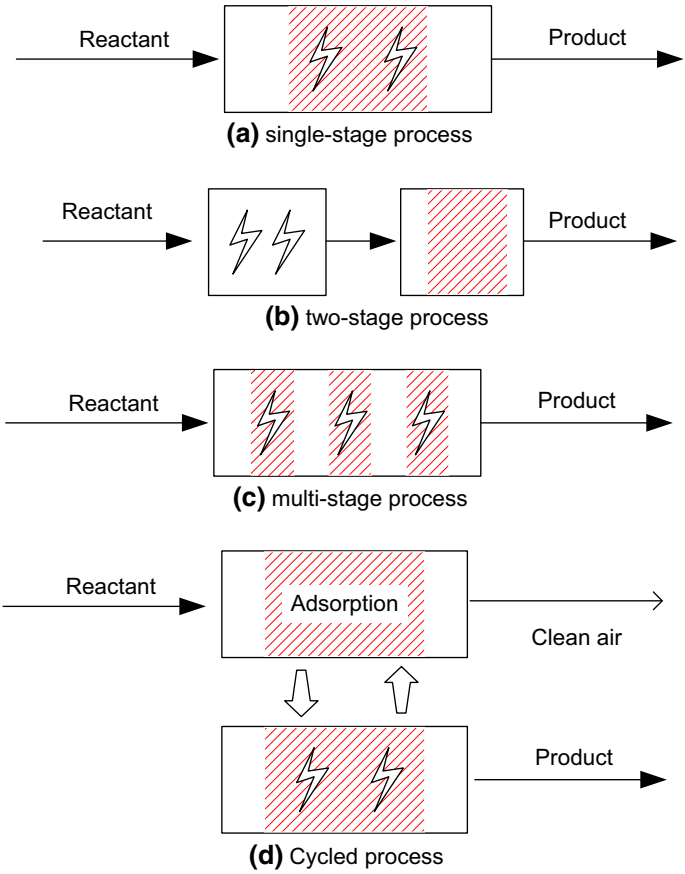

Fig. 2 Types of plasma-catalyst reactors according to catalyst bed the position and number

achieved separately in the two-stage process, and the majority of commercialized processes adopt a two-stage configuration. In contrast, complex interactions between NTPs and catalysts occur in single-stage processes, but current understanding of the fundamental elementary steps in such a reaction is still far behind that of the two-stage system. The position of catalysts is an important factor determining the performance of plasma-catalysis. Some catalysts (for example, MnO_2, and Ba-CuO-Cr_2O_3/alumina) are better as two-stage than as single-stage [74–76]. In many cases, single-stage configuration has been found to be better than two-stage (including ozone injection) for a given catalyst [33, 77–82]. A multi-stage system (c) is an interesting option for the industrial use of plasma-catalysis in the future. The most interesting aspect is that each catalyst has a different function, in accordance with its position and the expected reaction [83]. Several combination types may be possible, for example: "initial breakdown of precursor → deep oxidation of intermediates → O_3 killer catalyst" [84]. Hubner et al. [85] have studied ethylene (C_2H_4) destruction using a three-stage reactor packed with glass beads (6 mm in diameter). They found that the destruction efficiency was influenced by the specific energy input only, rather than the number of stages; this may have primarily been due to the nature of the packing material (glass beads). In addition, the formation of harmful byproducts was reduced with an increased number of stages. Harling et al. [86] have reported a multi-stage system for cyclohexane (C_6H_{12}), and toluene (C_7H_8) removal. In that case, the reactor was composed of three plasma reactors followed by two catalyst beds (MnO_2/alumina honeycomb, MnO_2-CuO).

Cycled system (d) consists of two steps of adsorption and plasma decomposition of adsorbed pollutants. Sivachandiran et al. [87] indicated that the cycled system decomposed isopropanol (IPA) using 14.5 times less energy than the continuous treatment. Further, direct plasma has exhibited superior performance to O_3 injection in the removal of adsorbed IPA [88]. Oxygen plasma is an interesting option for the plasma decomposition of adsorbed pollutants [89–92]. First, NOx formation can be completely suppressed by the oxygen plasma. Second, the decomposition rate is significantly increased for oxygen plasma compared to air plasma at the same power input, which is rarely observed in plasma-alone processes [90]. As technical progress continues, finely-tailored plasma-catalysis reactors will be further developed in the future.

The majority of plasma-catalysis reactors are operated in the presence of at least one barrier, so as to prevent arc formation. Catalysts are represented as capacitors and resistors in plasma catalysis equivalent circuits [72]. When barrier discharge plasma reactors (including catalysts-packed reactors) are operated at high temperatures (usually >373 K), the discharge characteristics are altered. The electrical discharge tends to become unstable as the temperature increases [93], and these effects can be easily observed in the V–Q Lissajous figure, the shape of which changes of from a parallelogram to an ellipse [94, 95]. This is because the load characteristic of a barrier or catalyst becomes more resistive than capacitive. In contrast to AC corona discharges (i.e., without a barrier), typical barrier discharges have a 90° phase difference between the discharge current and applied voltage, which is also good evidence of the capacitive nature of barrier discharges. The capacitor (C_m) for measuring charge (Q) should have larger capacitance than the dielectric barrier (C_d), to avoid any interference in the circuit ($C_m/C_d > \sim 1000$). The electrical conductivities of a dielectric barrier and catalyst increases with temperature, which can result in a substantial change in the overall equivalent circuit of the plasma reactor [95]. It has also been reported that a V–Q Lissajous figure with an ellipse shape can be obtained for a CO_2 laser operated at room temperature, large gaps (0.4–0.8 mm), and a frequency of 100 kHz [96, 97], where ions can be trapped in the discharge gap. This behaviour must therefore be

monitored closely, especially when a plasma-catalysis reactor is operated at high temperature and/or high frequency.

Key Components of Plasma

Figure 3 shows the six key elements of plasma: electrons, photons, neutrals, excited molecules, and positive and negative ions. Basically, plasma chemistry involves the combined interactions of these components, regardless of the application types. The effect of plasma on catalysts can also be explained by considering the roles played by each of the components. Electrons are easily accelerated under an electric field because of their small mass, and they play a pivotal role in plasma generation. Plasmas are often classified as "thermal" and "nonthermal" based on the temperatures of the electrons (T_e), ions (T_i), and neutral molecules (T_g). A plasma satisfying the condition $T_e \gg T_i \approx T_g$ is labelled as NTP. Ultraviolet (UV) radiation is primarily generated from the NO γ-band (236 nm), the OH ($A^2\sum^+ \rightarrow X^2\prod$, 306–312 nm), the second positive band of N_2 (337.1 nm), and the first negative band of N_2^+ ions (391.5 nm) in air-like mixtures. Quantitative measurement of the UV flux in an atmospheric-pressure NTP has revealed that the flux has a range of only several μW/cm^2 [98, 99], which is even smaller than that of outdoor sunlight (several mW/cm^2). Photocatalytic reactions usually occur at a space velocity below $\sim$100 h^{-1}, which is 2–3 orders of magnitude smaller than that in plasma-catalysis (>10,000 h^{-1}). Thus, many different groups have reached similar conclusions, i.e., that UV-induced catalytic reactions are negligible in plasma-catalysis [100–102]. However, UV irradiation on the reactor surface may assist plasma generation through the Joshi effect [103, 104]. It is well-known that external UV-irradiation of a plasma reactor enhances plasma intensity or the number of microdischarges [105–107]. This kind of interaction may be possible locally within the scale of microdischarges, and detailed study to elucidate the bilateral interactions is necessary.

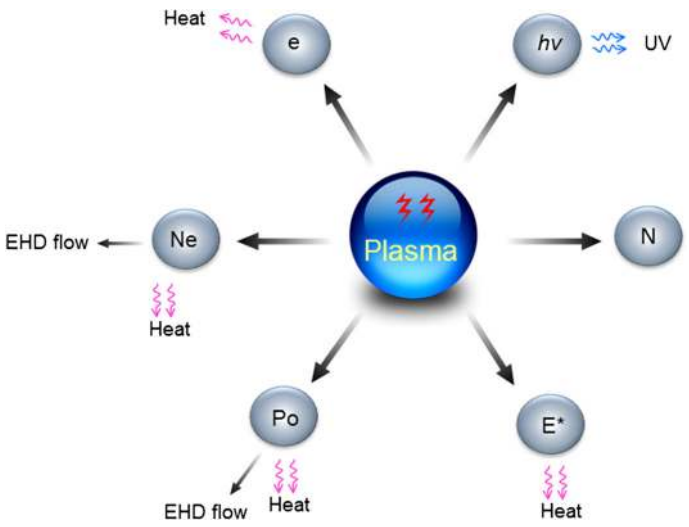

Fig. 3 Six major components of plasma; e = electron; hv = photon; N = neutral (molecule or atom); E* = excited molecule; Po = positive ion; Ne = negative ion

A possible secondary effect in plasma is the generation of electrohydrodynamic (EHD) flow, which is often referred to as corona or ionic wind. Ions drifting along the discharge channel transfer their energy to the colliding gas molecules, thereby generating a gas flow [108]. The velocity of the EHD flow is a square root function of the discharge current ($V_{EHD} \approx K\sqrt{I}$), where K is a constant depending on the electrode configuration. The typical value of V_{EHD} is $\sim$10 m/s [109–112]. This EHD flow may create turbulent conditions near the catalyst bed, and promote mass transfer from the gas-phase to the surface. The presence of EHD flow can certainly play a role in the mass transfer of both reactants and long lived active species of O_3 and excited molecules. Kanazawa et al. [113] studied NO removal using a two-dimensional (2D) laser-induced fluorescence (LIF) technique, and visualized the expanding reaction zone against the main gas flow.

The current flow induced by the migration of charged species (electrons and ions) will induce a temperature increase in the reactor through joule heating, dielectric loss, and gas heating in the plasma channel. The dielectric loss increases with the dielectric constant, so the presence of ferroelectric materials ($BaTiO_3$) tends to increase the reactor temperature more easily [114]. The low O_3 generation in a $BaTiO_3$–packed bed ($\varepsilon_s > 2600$) is a good example of this trend [115]. The temperature increase (ΔT) depends primarily on the energy input in the reactor, and therefore, more careful attention is required when the reactor is operated at a high power input. Temperature is also an important factor in the design of chemical reactors. Chemical reactions can be classified into "exothermic" and "endothermic" reactions depending on the enthalpy changes (ΔH). Table 2 summarizes some of the representative reactions usually considered in plasma chemistry. In thermodynamics, an endothermic reaction is described as a process in which heat is absorbed from the system and ΔH becomes positive ($\Delta H > 0$). In contrast, an exothermic reaction releases heat so that ΔH has a negative value ($\Delta H < 0$). The change of temperature in a system induces a change in equilibrium. Le Chatelier's principle states that exothermic and endothermic reactions favor low and high temperatures, respectively. O_3 generation (R5, Table 2) is an important example of an exothermic reaction ($\Delta H = -22.7$ kJ/mol) that follows this principle. O_3 yields in nonthermal plasmas reach 150–250 g-O_3/kWh in air and 300–550 g-O_3/kWh in O_2 [116], but only 2 g-O_3/kWh in inductively coupled plasma (ICP) torch [117]. The thermodynamic nature of the O_3 generation justifies the use of cooling system in the majority of industrial ozonizers well. Another exothermic process of methanol synthesis over Mo-CuO/Al_2O_3 exhibits a peak at 150 °C and decreases with a further increase in temperature [118]. Dry (R1, Table 2) and steam reforming (R2, Table 2) are highly endothermic processes. In contrast to O_3 generation, a gliding arc or heat-insulated reactor can be a sensible option for the endothermic reactions. Gliding-arc and arc discharge have been shown to exhibit significantly better performance in R1 or R2 than NTP (DBD or pulsed discharge) [119, 120]. Methane (CH_4) reforming using plasma-catalysis is usually conducted at high temperature, which reflects the thermodynamic nature of the reactions well.

Role of Plasma in Three Key Catalysis Steps

Figure 4 is a schematic diagram of the three successive key steps in a catalytic reaction: adsorption, surface reaction, and desorption. The presence of a catalyst reduces the activation energy by providing new pathways in the chemical reaction. This effect is often observed in VOC oxidation, through comparison of the temperature window with and without a catalyst. One of the interesting roles of a catalyst is the ability to provide a new

Table 2 Representative chemical reactions and their changes in enthalpy

Reaction		Enthalpy changes (ΔH)	No
Endothermic			
$CH_4 + CO_2 \rightarrow 2CO + 2H_2$	Dry reforming	247.4 kJ/mol	R1
$CH_4 + H_2O \rightarrow CO + 3H_2$	Steam reforming	206.3 kJ/mol	R2
$CH_4 + 2H_2O \rightarrow CO_2 + 4H_2$	Steam reforming	165.3 kJ/mol	R3
$H_2 + CO_2 \rightarrow CO + H_2O$	Reverse water–gas shift reaction	41.2 kJ/mol	R4
Exothermic			
$O + O_2 + M \rightarrow O_3 + M$	Ozone generation	−22.7 kJ/mol	R5
$CH_4 + 1/2O_2 \rightarrow CO + 2H_2$	Partial oxidation	−35.6 kJ/mol	R6
$CO + H_2O \rightarrow H_2 + CO_2$	Water–gas shift reaction	−41.2 kJ/mol	R7
$CO_2 + 3H_2 \rightarrow CH_3OH + H_2O$	Methanol synthesis	−49.5 kJ/mol	R8
$N_2 + 3H_2 \rightarrow 2NH_3$	Ammonia synthesis	−92.4 kJ/mol	R9
$CO + 2H_2 \rightarrow CH_3OH$	Methanol synthesis	−128 kJ/mol	R10
$CO_2 + 4H_2 \rightarrow CH_4 + 2H_2O$	Sabatier reaction (methanation)	−164.8 kJ/mol	R11
$CO + 3H_2 \rightarrow CH_4 + H_2O$	Methanation	−205.8 kJ/mol	R12

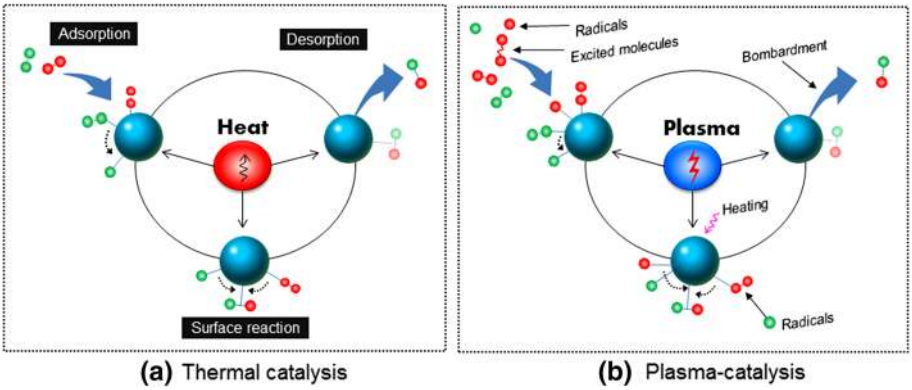

Fig. 4 Three key steps in (**a**) thermal catalysis and (**b**) plasma-catalysis

reaction pathway, which eventually leads to reduced activation energy and higher reaction selectivity. For example, the bonding energy of nitrogen in gas-phase is 9.8 eV. This bond energy has been shown to decrease to 5.46 and 4.92 eV on the hexagonal close-packed (hcp) and face-centered cubic(fcc) sites of ruthenium (Ru), respectively [121]. Plasma can be substituted in place of heat, but its effect is somewhat different to thermal catalysis. The extent of adsorption is inversely proportional to the temperature, so the low operation temperature of plasma-catalysis is beneficial. Further, plasma can provide two additional chemical functions for adsorption. First, plasma generates reactive radicals and excited molecules. When molecules are dissociated by the electron impact in plasmas, the resulting atoms become electrophilic as a result of the unpaired electrons. Radicals may promote their adsorption onto the electron-rich surfaces. The excited molecules can be dissociated on the surface more easily than the ground-stage molecules. The importance of the excited molecules to this process is evidenced by the increased cross section and the shift of the

threshold to a lower energy level. In fact, Burrow has indicated that the dissociative cross section of O_2 ($a^1\Delta_g$) is approximately three times larger than that of the ground stage O_2 ($X^3\sum_g$) [122]. The reaction rate constant of N_2 (A) is also known to increase by approximately 2.3 fold as the vibration level is increased from $v = 0$–3 [123]. Nozaki et al. [124, 125] have shown that vibrationally excited CH_4 can improve dissociative chemisorption onto a Ni surface. Second, some reactant components are converted into intermediates by radicals in the gas-phase, which are often adsorbed more easily than the parent molecules. The fixation of oxygen radicals and nitrogen radicals has been demonstrated via isotopically-labelled probe molecules ($^{18}O_2$) and titration techniques [126–129]. Ag nanoparticles on TiO_2 or zeolite provide adsorption sites for surface oxygen species [130]. Adsorption can also change the plasma-catalysis reaction, because dilute reactants are concentrated on the surface. Oh et al. [131] have indicated that the toluene decomposition rate increases by a factor of $\sim$3.6 depending on the position of zeolite, for a plasma-catalysis reaction. Dissociatively chemisorbed species move on the surface via spillover (generally from metal to support) or surface diffusion, which eventually occurs in surface reactions. O_3 can be dissociated on the surface of a metal and form surface oxygen species (M*O) via

$$O_3 + M^* \rightarrow M^*O + O_2 \quad \text{(R13)}$$

$$M^*O + \text{reactants} \rightarrow \text{products} + M^* \quad \text{(R14)}$$

where M* denotes an adsorption site. The M*O reacts with the adsorbed target molecules (R14), as has been observed for many reactions in O_3-assisted catalysis. However, some of the M*O catalytically decompose O_3 (R15) and the eventually increases the O_3 demand factor. In 1920, Rideal and Kunz proposed Ag_2O as Ag*O for the decomposition of O_3 [132]. Further, Li et al. [133] demonstrated that the Eley–Rideal (E–R) process of O_3 decomposition on a Mn catalyst using isotopic exchange can be expressed as;.

$$O_3 + Ag^*O \rightarrow Ag^* + 2O_2 \quad \text{(R15)}$$

Ag/ZSM-5 exhibits high activity toward O_3 decomposition, but its contribution to toluene (C_7H_8) removal is weak [83]. As mentioned in subsection "Catalytic Actions in the Corona Electrode", however, Ag is active in the catalytic ozonation of CO. The different behaviors of Ag in different reactions may partially arise from discrepancies between the reaction sites in each reaction.

Plasma-induced radicals can attack the adsorbed molecules directly (i.e., the E–R mechanism). As an example of these E–R like reactions, note that CO has been oxidized over a fully deactivated Au/TiO_2 catalyst in the presence of plasma [82]. In contrast to the conventional E–R reaction, where the active species are fixed on the surface, this gas-phase radical-induced process can be referred to as a *reverse E–R reaction*. Further, O_3-assisted catalysts constitute additional evidence of the E–R type reaction. Toluene decomposition has been observed on a bare HY zeolite, which is almost immune to O_3 [134]. Plasma can also promote the desorption process through ion and electron bombardment. Yamamoto et al. reported plasma-induced desorption of water molecules [135], CO_2 [136], and NOx [137, 138]. Desorption can be a rate-limiting step because the plasma-catalysis is generally conducted at a temperature that is far less than that of the thermal catalysis. Plasma can therefore interact with surface at each elementary step with different functions.

Figure 5 compares the characteristic time-scales in plasma and catalytic reactions. The chemical reactions in plasma can be divided into fast (radicals) and slow (O_3 and H_2O_2) reactions, which are usually observed after the streamers have disappeared. Ion chemistry

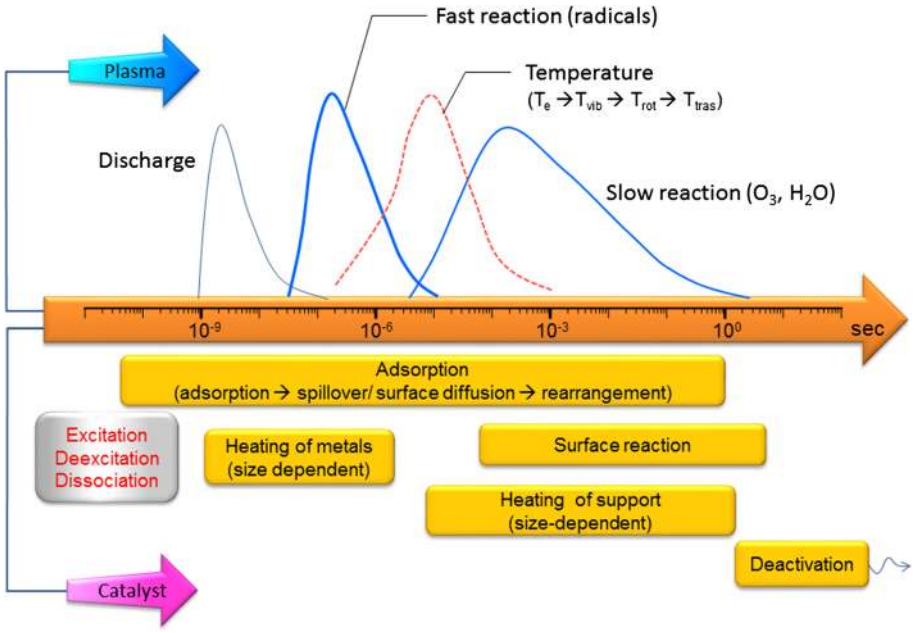

Fig. 5 Characteristic time-scales in plasma and catalytic reaction

(ion-molecules) proceeds even faster than radical reactions, but their direct contributions to the overall reaction are considered to be negligible [124]. In a catalytic reaction, the initial chemisorption step occurs within 10^{-9} s. However, the total adsorption process proceeds over a significantly longer time scale (up to 10° s), as a result of surface rearrangement via spillover and surface diffusion, along with gas-phase diffusion into the micropores. The catalytic turnover time-scale is known to be in the range of 10^{-2}–10^{2} s [139], which is slower than the fast radical reactions by a factor of 2–3 orders of magnitude. This different time-scale suggests that the rate-limiting step is a surface reaction rather than a plasma-involved process in the gas-phase. In other words, the chemical reaction proceeds in one direction from the plasma to the catalyst, and not vice versa.

Whether or not heating in the plasma can contribute to plasma-catalysis is a point of contention. The temperature increase in plasma-catalysis is basically a function of the input energy. Figure 6 shows temperature increase profiles of catalysts after the plasma is turned on. An infrared camera (NEC/Avio, TVS-500EX with TVS-25 μm lens) with a time resolution of 20 frames per second was used to track the temperature change. The temperature on the measurement area increases rapidly for a period up to 2 min and then began to level off. The rotational temperature in a plasma channel reaches up to 400–1000 K depending on the input power, gas composition and the type of plasma reactor [140–142]. The transitions of a vibrational–vibrational (V–V) and a vibrational—translational (V–T) temperature occur within $\sim 10^{-4}$ s in a post-discharge period. The presence of humidity accelerates the V–T transition rates of O_2 and N_2 [142–144]. The open question here is whether these transition temperature changes affect the catalyst heating and the catalytic reaction. The time-scales of the Ag (10 nm) and support (2 mm, the size of catalyst pellets) heating have been estimated to be approximately $\sim 10^{-12}$ s and 5 s, respectively. This different time-scale indicates that the Ag can be heated or cooled more rapidly than the

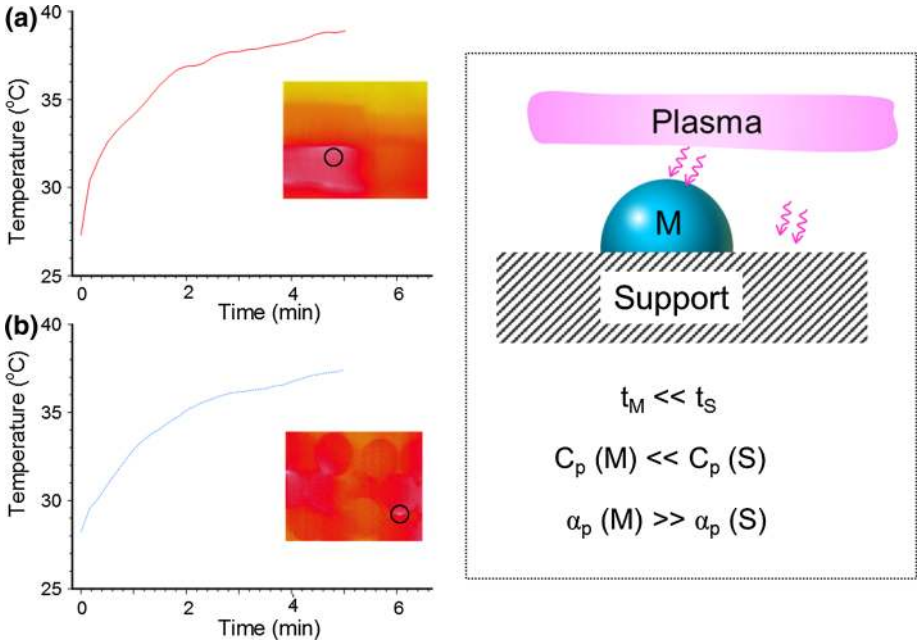

Fig. 6 Temperature increase of catalyst bed under plasma application: **a** 10 wt% Ag/MOR: **b** 2 wt% Ag/TiO_2. The circles in the inset figures indicate the position of temperature measurement. The applied AC voltage and frequency are 14.5 kV and 1 kHz, respectively. C_p, t and α represent heat capacity, heating time and thermal diffusivity, respectively. The M and S supscripts indicate metal and support, respectively

supports. However this time-scale does not agree with the aforementioned catalytic turn-over time-scale. These fast interactions in plasma-catalysis are still in black box, and further investigation is required.

Fundamental studies on the interaction between NTP and catalysts are often limited by the lack of available instruments, especially for in situ measurements. The presence of electrical discharge, electrical insulation, and electromagnetic noise causes difficulties in applying the well-established techniques commonly used in the thermal catalysis investigations, such as Fourier transform infra-red (FTIR) spectroscopy, X-ray photon spectroscopy (XPS), electron spin resonance (ESR) spectrometry, X-ray diffraction (XRD), operando scanning tunnelling microscopy (STM), and Raman spectroscopy. Recently, in situ ESR was implemented in low-pressure plasma sterilization [145, 146]. LIF technique can also be implemented in plasma-catalysis. For example, Su et al. applied LIF for high throughput screening of catalysts. They positioned fifteen different catalysts on a plate and introduced a laser sheet close to the surface. Then they monitored the reaction product of naphthoquinone (488 nm for excitation and 515–545 nm for fluorescence), which was produced from naphthalene over a vanadium oxide (V_2O_5) catalyst [147, 148]. The LIF technique was also found to be effective for detection of the OH radical and N_2(C) near the surface discharge plasma [149]. Aydil et al. [150] reported in situ monitoring of the surface passivation of silicon (Si) and gallium arsenide (GaAs) using attenuated-total-reflection FTIR (ATR-FTIR) spectroscopy. Aissa et al. [151] reported on the thermal conductivity of AIN during pulse laser deposition using IR operando spectroscopy, with a time resolution of approximately 10^{-8} s. Implementation of these techniques and/or additional refinement

of in situ monitoring techniques may further accelerate the progress of plasma-catalysis technology.

Effective Catalyst Selection Strategy for Plasma

How can we Choose the Right Catalyst for Plasma?

The history of this research field is relatively short, and a general rule for selecting the appropriate catalyst for a particular plasma-catalysis reaction has not yet been established. Catalysts are essentially combinations of active transition metals and supports (such as titania, alumina, silica, activated carbon and zeolite); therefore, the number of catalysts are myriad. Furthermore, various methods exist for the preparation of each combination. The precursor type is also known to affect the catalytic performance. Different researchers have tested different catalysts, and even attempted different reactions under different conditions. One simple and straightforward approach to determining the appropriate catalyst for a particular reaction is to use an accumulated database on thermal catalysis. For example, Ni is a well-known catalyst in CH_4 reforming and has also been tested by many research groups with regard to plasma-catalysis, specifically for the dry reforming of CH_4 [81, 124, 152, 153] and the methanation of CO and CO_2 [154]. CO oxidation over gold (Au) nanoparticles was first demonstrated by Haruta, and was even conducted at low temperature (200 K) for Au nanoparticles with <10 nm diameter deposited on an oxide surface (i.e., TiO_2, Co_3O_4, Fe_2O_3) [155–157]. This reaction was also found to be effective in plasma-catalysis [82]. Oxygen plasma can successfully regenerate deactivated Au/TiO_2 [82, 158], but N_2 containing plasma causes further deactivation because of the formation of surface nitrogen oxides [158].

Chemisorbed O_2 molecules form metal-atomic oxygen (M–O) bond until they are consumed by reactions. For the meal catalyst to be reactive, the M–O bond energies should be low. Figure 7 summarizes the M–O bond energies reported in the literature [159–161]. The order of the M–O bond energies reflects their catalytic activities for the majority of oxidation reactions well; further, the M–O bond energy also differs in accordance with the surface site. For example, Pt (111)–O bond energies vary according to the adsorption sites, being 4.15, 3.08, and 3.01 eV for one-fold site, bridging, and high-coordinate sites, respectively [162]. Cluster catalysts are also an important topic in recent studies of catalysis. The reaction rate and selectivity change dramatically in accordance with the magic number of the metal clusters. Turner et al. [163] have reported the selective oxidation of styrene with O_2 on the Ag55 clusters supported on inert support.

Surface Streamers and Catalytic Performance

A strong relation between the propagation of surface streamers and the catalytic performance in single-stage plasma-catalysis of VOC has been observed [164, 165]. Intensified charge-coupled device (ICCD) camera imaging of plasmas on catalysts has indicated that there are two different discharge modes. Partial discharge is usually observed in the vicinity of contact points between catalysts. As the applied voltage is increased, plasma is observed not only at the contact points (partial discharge), but also on the surface of the catalysts. In the case of $BaTiO_3$, which has a relatively large ε (1000), only partial discharge occurs and the area of discharge is increased with increased applied voltage.

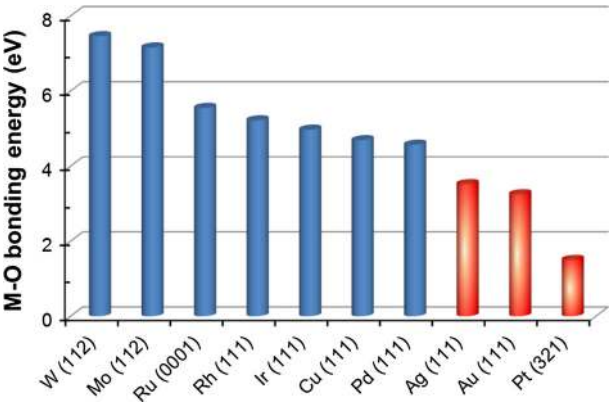

Fig. 7 Binding energies of metal–oxygen atom. The coverage of W and Mo is 0.5 ML and that of the remaining elements is 0.25 ML

However, plasma does not propagate to the surface. For catalysts to be effective in plasma, the contact area should be as large as possible, which is a prerequisite for strong interaction. To utilize the short-lived radicals effectively on the surface, the distance between the plasma and catalyst should also be as small as possible. The dimensionless parameter Λ has been introduced in order to describe the criteria of direct interactions between plasma and catalysts [72].

$$\Lambda = \frac{l}{L_D + L_{ef}} \leq 1 \tag{1}$$

Here the L_D and L_{ef} represent the diffusion length of the reactive species and the migration length of the ionic species, respectively. Λ can also be applied to the other plasma processes (plasma sterilization/medicine and surface treatment) that require the transport of short-lived species from the plasma to the target media.

From an electrical perspective, catalysts have the electrical components of resistivity, capacitance, and dielectric constant. When these materials are packed in a plasma reactor, the overall equivalent circuit changes in accordance with each of these values, which affects the plasma generation. The experimentally confirmed changes in the plasma generation are as follows: (1) decreased plasma onset voltage [166], (2) increased number of microdischarges, and (3) extension of the plasma area by the loading of metal nanoparticles on the surface [164]. Recently, we studied the effect of the silica and alumina ratio on the plasma generation in the case of Ag supported HY zeolite [165],with all else being constant. The Ag/HY catalyst with a low Si/Al ratio exhibited superior performance both in terms of activity and streamer propagation. The Ag state and the resultant changes in the electrical resistivity were found to be important factors in this regard. An optimum range of electrical resistivity in catalysts exists, which should be investigated in detail in future studies. Recently, fluorescence from the plasma-excited Ag/HY catalyst has been observed, which is also good evidence for the direct interaction of plasma with the catalyst surface [165, 167].

In recent years, interesting experimental data have been reported for the enhanced dissociation of adsorbed molecules through external electron injection via a bias-voltage

[168] or the tip of scanning tunnelling microscopy (STM) [169]. Deshlahra et al. have studied the CO bond on the Pt–TiO_2 Schottky junction using the multilayer enhanced infrared reflection absorption spectroscopy (MEIRAS) technique. They successfully controlled the red- or blue-shift of the adsorbed CO by adjusting the bias-voltage (within only ±2 V) applied to the Pt–TiO_2 junction. Lee et al. studied the electron-induced dissociation of adsorbed CO_2 on TiO_2 (110) with O_2 vacancy defects. They injected electron via STM tip and confirmed the enhanced dissociation of CO_2. They reported the threshold energy for this process to be 1.4 eV above the conduction band of TiO_2. In plasma-catalysis, where the surface streamers propagate on the catalysts surface, the accumulation and relaxation of charged species (i.e., electrons and ions) always occurs within a time-scale of $\sim 10^{-8}$ s. It is interesting to determine whether this low voltage-induced surface process is also possible in plasma-catalysis.

Durability is also a key factor as regards practical application of plasma-catalysis. The majority of plasma-catalysis studies have so far been conducted on the laboratory-scale, and long-term testing (typically exceeding several thousand hours in duration) has not yet been reported. For benzene (C_6H_6) decomposition over a Ag/TiO_2 catalyst, a stable operation has been observed under the continuous operation for 150 h [170]. Several different catalyst deactivation mechanisms exist: sintering (nanoparticles aggregation), poisoning (due to P, S, Cl, Hg, Pb), carbon deposition, and thermal or mechanical stress [171]. Carbon (coke) deposition has also been observed in the plasma CO_2 reforming of CH_4 over a Ni catalyst [172]. The low operating temperature of plasma-catalysis may be beneficial for the suppression of sintering. Furthermore, plasma treatment has also proven to be efficient as regards the size reduction of active metals [173]. Further, Zou et al. [174] applied glow discharge to modify Pt-doped TiO_2, and found that the plasma treated catalyst was more active in H_2 generation. They ascribed the improved performance to the enhanced Pt-support interaction rather than dispersion.

Plasma generation and the catalyst surface conditions interact bilaterally. This is because plasma alters the surface conditions including the redox of metal nanoparticles, and the catalyst conditions largely affect the characteristics of plasma. A multidisciplinary approach is therefore necessary in order to elucidate the working mechanisms in plasma-catalysis.

Environmental Treatment Application

Recently, many review papers on VOC removal using plasma-catalysis have been published [175–180]; therefore only brief remarks will be given here. The formation of NOx (NO and NO_2) or acids (HNO_2 and HNO_3) is one of the important issues concerning the removal of VOC in air. The removal rate is essentially dependent on the energy input, so the higher the initial VOC concentration, the higher the required energy input. The use of a catalyst can suppress the NOx formation to some degree, but complete suppression is difficult so long as the plasma reactor is operated in air. NTP alone is only capable of chemically reducing NOx to N_2 when the O_2 content is lower than approximately 3–5 % [181–184]. The critical oxygen content, defined as the O_2 content at which net NOx reduction occurs in NO/O_2/N_2 mixtures, increases with increased initial NO concentration (e.g., 100 ppm NO at 1.1 % O_2, 1000 ppm NO at 5.5 % O_2) [185]. In plasma-catalysis, there are two possible approaches to solve this NOx problem. One is the use of O_3-assisted catalysis, where the plasma is only used for O_3 generation in O_2 [186], whereas the other

method is the cycled system consisted of adsorption and oxygen plasma. VOCs are first adsorbed on the catalyst without plasma application, and the VOCs-saturated catalysts are then treated with plasma after the catalyst bed is purged with O_2 [89]. This cycled system has been proven to be effective for C_6H_6 [90, 91], C_7H_8 [92, 187], and formaldehyde (HCHO) [188]. These two methods share a common idea, in that the plasma is turned on in an oxygen environment. In Japan, several commercial-scale ($\sim$up to 60,000 Nm^3/h) plasma-catalyst systems are in operation [189]. However, the majority of these systems are designed for odor removal, where the typical concentrations are below several parts per million by volume (ppmv). The operating specific input energy is also only 1.1 J/L, which is definitely free from NOx formation, based on the emission standard regulations. One of the important applications of plasma-catalysis is indoor air cleaners [190]. Annual sales of these devices exceeded 2.5 million in Japan in 2011 and 4 million in China in 2014. In Japan, the majority of these cleaning devices utilize plasma-based technology.

Plasma-involved selective catalytic reduction (SCR) processes (i.e., two-stage process) for the NOx removal have also been studied intensively [191, 192]. WO_3–V_2O_5/TiO_2 catalysts are usually used for such applications because they have been well studied with regard to the conventional selective-catalytic reduction (SCR) process. NH_3 has been used as a reductant (i.e., NH_3-SCR), because of its high reactivity and low working temperature compared to hydrocarbons (i.e., HC-SCR). The V_2O_5/TiO_2 catalyst has good activity toward the NH_3–NO (R16) system but is less reactive to NO_2 (R17). In a two-stage process, plasma converts NO into NO_2 (R18) with relatively low energy input, and the NO/NO_2 mixtures are subsequently treated in the catalyst bed [38, 191, 193, 194]. The reaction of NO–O_3 is selective even in NOx–SOx–COx–HC mixtures [195–197], so the O_3 injection can also be used for selective oxidation of NO. The presence of hydrocarbon (mostly olefins) facilitates the conversion of NO into NO_2 in plasma chemistry (R19 and R20) [198]. The key aspect of this conversion the formation of peroxide radicals (HO_2, RO_2), which are effective for NO oxidation over a wide temperature range. In many cases, catalysts are more active to NO_2 than NO, so R17 is referred to as the "fast SCR" reaction [199]. Koebel et al. [200] have shown that the reaction rate of fast SCR is ten times higher than that of the standard SCR reaction. Stevenson and Vartuli have reported that NO_2 reduction proceeds one hundred times faster than NO reduction over an HZSM-5 catalyst. The optimum ratio of NO:NO_2 in NH_3-SCR is approximately 1:1 [38, 40, 194]. Two important issues in NH_3-SCR are the NH_3 slip and the formation of ammonium nitrate aerosol (NH_4NO_3). NH_3-SCR over a V_2O_5/TiO_2 catalyst has exhibited fast deactivation due to the formation of NH_4NO_3 [201, 202]. On the other hand, Cr_2O_3/TiO_2 and Co-ZSM5 have exhibited stable performance without aerosol formation [37, 202].

$$4NO + O_2 + 4\,NH_3 \rightarrow 4N_2 + 6H_2O \quad \text{(R16)}$$

$$NO + NO_2 + 2\,NH_3 \rightarrow 2N_2 + 3H_2O \quad \text{(R17)}$$

$$NO + O \rightarrow NO_2 \quad \text{(R18)}$$

$$NO + HO_2 \rightarrow NO_2 + OH \quad \text{(R19)}$$

$$NO + RO_x \rightarrow NO_2 + RO_{x-1} \quad \text{(R20)}$$

NOx removal from mobile sources (cars and trucks) requires a more complex considerations such as fuel penalty, energy consumption and the supply of reducing agent. A three-way catalyst is no longer effective for diesel flue gas, because of the high oxygen content

(5–15 %). Two possible lean-NOx catalyst options for diesel application are urea and HC-SCR. As a result of the pioneering work by Iwamoto concerning NOx removal in the presence of O_2 using Cu ion exchanged-ZSM5 zeolite, the use of hydrocarbon as reductants has attracted considerable attention [203, 204]. However, a significant disadvantage exists in that the HC-SCR process requires a higher temperature (usually > 573 K) than the NH_3-SCR process. Plasma can convert HC into aldehydes, which can play an important role in the HC-SCR process [37, 205–207]. Penetrante has reported HC-SCR of 500 ppm NOx at 573 K and 36 J/L [191]. Acetaldehyde has also been found to be effective for NOx removal in a single-stage plasma-catalysis using γ-Al_2O_3 at 423 K [208]. For the application for cars, reductants can be supplied by on-board reforming of fuels [209]. The desirable reforming products are aldehydes and H_2 which have also been found to be effective in conventional SCR process. The process using H_2 as reducing agent is called as H_2-SCR process [210]. The ideal reaction is R21 but N_2O formation (R22) also occurs as a side reaction [211].

$$2NO + 4H_2 + O_2 \rightarrow N_2 + 4H_2O \quad \text{(R21)}$$

$$2NO + 3H_2 + O_2 \rightarrow N_2O + 3H_2O \quad \text{(R22)}$$

$$NO + 5/2H_2 \rightarrow NH_3 + H_2O \quad \text{(R23)}$$

The hydrogen as reductant is prominent on Ag, and H_2 is converted into NH_3 on the surface (R23), which eventually takes part in the NOx reduction. Lee et al. [212] reported an interesting results that plasma reformed reductants was more reactive in de-NOx than the injection of gas mixture with similar composition. Cycle system has also been applied in NOx removal processes [213]. Desorbed NOx from the saturated adsorbents can be treated with N_2 plasma [137, 138, 214]. Wang et al. [215] used CH_4 plasma for the reduction of NOx, which was adsorbed on H-ZSM-5 zeolite (Si/Al ratio = 22). The performance was stable up to 6 reaction cycles.

$$\begin{aligned} NOx\ (NO \gg NO_2) &\rightarrow NOx\text{-adsorbent (adsorption)} \rightarrow NOx\ (\text{desorption}) \\ &\rightarrow N_2(N_2\text{plasma}) \end{aligned} \quad \text{(R24)}$$

Leray et al. [216] have demonstrated that a two-stage plasma-assisted system provides lower light-off temperatures for the oxidation of CO and hydrocarbons (HCs) over Pt–Pd/Al_2O_3 diesel oxidation catalyst (DOC).

Energy Application (NH_3 Synthesis)

Historical and Social Context of Ammonia Production

As shown in Fig. 1, the energy-related applications of plasma-catalysis include dry reforming of CH_4 [81, 152, 172, 217, 218], fuel reforming for engines, etc. [219–225], syngas production [226–228], H_2 formation [229–234], methanol synthesis [118, 235, 236], and methanation [154, 237]. These topics will not be discussed further here. Instead, we focus on NH_3 production as a potential application of plasma-catalysis.

NH_3 is used as a feedstock for various industrial chemical products such as nitric acid, resins, dyes, pharmaceuticals, fertilizer, synthetic textile fibres and plastics. Recently, NH_3 has been attracting attention as a potential H_2 carrier for long distance transport or storage, because it can be easily liquefied under mild conditions (293 K, 0.8 MPa). Considering the

large minimum ignition energy of NH_3 (680 mJ) compared to that of H_2 (17 μJ in dry air) [238, 239], NH_3 has therefore a strong beneficial for safe storage including long distance transport. Liquid NH_3 also has a significantly narrower explosion limit than H_2 (16–25 % vs 18.3–59 % in air) [240]. NH_3 has a large mass density of H_2 (17.56 wt%), and easily converted back to hydrogen [241]. Unlike the other H_2 carrier candidates (such as methylcyclohexane) NH_3 is basically a carbon-free fuel.

The Haber–Bosch (HB) process has long been used to fix nitrogen and hydrogen to NH_3, being first introduced at the first industrial-scale demonstration (10 ton-NH_3/d) held at Oppau Germany in 1913. The HB process is a bellwether reaction in heterogeneous catalysis. Before the success of the HB process, there were strong concerns about the sustainability of human civilization, which were provoked by Thomas R. Malthus' publication, "Essay on the Principle of Population", in 1798. A hundred years after this serious question was first raised by Malthus, Sir William Crookes gave an historical speech at the British Association for the Advancement of Science (in Bristol) as follows:

> England and all civilised nations stand in deadly peril of not having enough to eat. As mouths multiply, food resources dwindle. Land is a limited quantity, and the land that will grow wheat is absolutely dependent on difficult and capricious natural phenomena… I hope to point a way out of the colossal dilemma. It is the chemist who must come to the rescue of the threatened communities. It is through the laboratory that starvation may ultimately be turned into plenty… *The fixation of atmospheric nitrogen is one of the great discoveries, awaiting the genius of chemist.* (*Chemical News V78, 125, 1898*)

Sir William Crookes is also famous for introducing the phrase "the fourth state of matter" to describe ionized gas (1879). This phrasing was used until Langmuir coined the term "plasma" in 1927. For many years, his memorable speech inspired many celebrated scientists, such as William Ramsay, Friedrich Wilhelm Ostwald, Walther H. Nernst, and Henry Le Chatelier to attempt NH_3 synthesis. In the Bunsen conference of 1907, it was concluded that industrial-scale NH_3 production is next to impossible; this consensus was based not only on lab-scale experiments but also on detailed discussions with engineers in the industry. However, Fritz Haber and Carl Bosch later accomplished this task using an alkali promoted Fe catalyst at high temperature ($\sim$500 °C) and high pressure ($\sim$30 MPa), via the so-called "HB process". The high temperature was required for activation of the catalyst, while the high pressure was necessary to shift the reaction equilibrium to NH_3. Figure 8 is a schematic diagram of the HB process. NH_3 synthesis (R9) is exothermal, so low temperatures are favorable in general. The dissociation of the triple bond of the N_2 molecule (9.8 eV) is usually considered as a rate-determining step in the HB process. The conversion rate in one pass is about 15 % and the unreacted gases are recycled to the catalyst bed. The catalysts are Fe promoted with K_2O or CaO and alumina. The HB process occupies approximately 3 % from the total world-wide energy consumption. The main drawback of the HB process is the large swings in pressure and temperature, which leads to the large energy consumption. H_2 for the HB process is supplied by hydrocarbon reforming, and the price of NH_3 primarily depends on the H_2 sources. During world war II, NH_3 was used as fuel for buses in Brussel for a year [242]. Later, sporadic studies on the use of NH_3 as an alternative fossil-based fuel had been conducted in some countries [243], but they did not received much attention because of the low cost of petroleum-based fuel. The large CO_2 emissions of 1.5–3.1 ton-CO_2/ton-NH_3 also increased the necessity for renewable energy-based H_2 production [244]. A possible renewable energy-based NH_3 production scenario involves the use of solar-powered H_2 production in sun-belt areas,

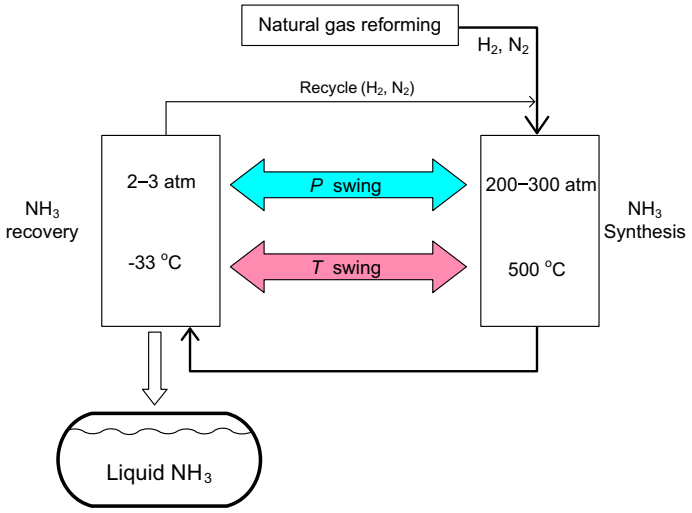

Fig. 8 Haber-Bosch process for NH_3 synthesis

followed by conversion into NH_3 before shipping, to facilitate long-distance distribution or storage.

The changing social and environmental conditions worldwide are creating significant scientific challenges and motivating the development of improved and more environmentally-friendly NH_3 synthesis processes using, for example, Ru catalysts [245, 246], C12A7 electride catalyst [247], steam electrolysis [248], and electrochemical cells [249–251]. Renewable energy-based H_2 production is also highly linked with environmentally-friendly NH_3 synthesis and the future hydrogen society. Most of the commercial HB process is usually operated for mass production of about 2000 tons-NH_3/day. However, the efficiency of this process is known to decrease, particularly when the plant size is decreased to about 100 tons-NH_3/day. If NH_3 production were matched to a renewable-energy-based distributed system (i.e., using solar power, wind power and so forth), the typical process size would be <10 tons-NH_3/day.

NH_3 Production Using Plasma-Catalysis

Kristian Birkeland and Sam Eyde invented an electrical arc plasma system for nitrogen fixation in 1903, the BE process, ten years before the HB process was invented [252, 253]. The energy consumption in the BE process was 15 MWh/ton-HNO_3, which corresponded to 67 g-HNO_3/kWh. Even though the BE process used renewable energy from a hydropower plant (Norsk Hydro Company), the energy consumption was considered to be extremely high. However, the BE process was soon replaced by the HB and Ostwald processes, primarily because of this large energy consumption. Recently, a large EU joint project called Microwave, Acoustic and Plasma Syntheses (MAPSYN) is aiming to achieve nitrogen fixation on an industrial scale [254–256]. Energy consumption and the consideration of energy efficiency are highly important topics for all kinds of applications using plasmas. Considering the exothermic nature of the NH_3 synthesis process, the low operating temperature of plasma-catalysis is attractive.

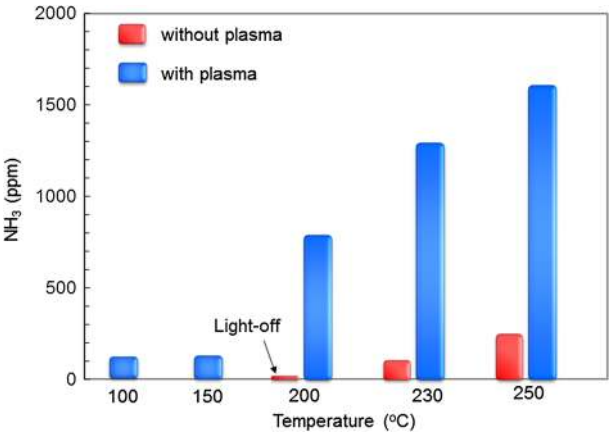

Fig. 9 NH_3 formation in Ru-Mg/γ-Al_2O_3 packed plasma reactor. The gas flow rate is 2 L/min with a ratio of N_2:H_2 = 8:2

The use of electrical discharges for NH_3 synthesis had been studied even before the Crookes's speech. According to the literature, Berthelot reported 3 % NH_3 production using a DBD reactor in 1876 [257]. Further, Wendt and Snyder operated a Pt wire-cylinder barrier reactor for 10–30 h and found the equilibrium concentration to be 4.1 % at atmospheric pressure [257]. Bai et al. [258] produced 8000 ppm of NH_3 from CH_4 and N_2 with an energy yield of 1.0 g-NH_3/kWh. They also reported that the yield increased by 1.54–1.75 times when MgO powders were used as the catalyst [259]. Electrical discharges coupled with catalysts had also been studied [260, 261]. Mizushima et al. [262] studied a metal loaded (Ru, Pt, Ni, Fe) membrane-like reactor for NH_3 synthesis, finding that Ru was most effective. Figure 9 shows NH_3 synthesis in a single-stage plasma-catalysis reactor packed with Ru-Mg/γ-Al_2O_3 pellets (3.2 mm diameter, 3.6 mm length) at different temperatures. When the temperature was below 150 °C, where thermal catalysis did not occur, the NH_3 yield was low at approximately 1.1–1.3 g-NH_3/kWh. Interestingly the effect of the plasma become prominent as the catalyst reached the light-off temperature. Approximately 10 ppm of NH_3 was observed at 200 °C with heating only, and the NH_3 concentration increased dramatically to about 810 ppm when the plasma was turned on (220 J/L). The same trends were observed at temperature up to 250 °C. In contrast to the stoichiometry of the HB process (H_2:N_2 = 3:1), the optimum ratio in the plasma-catalysis was found to correspond to nitrogen-rich conditions (H_2:N_2 = 1:4), which is consistent with other studies using plasma [259, 263].

Table 3 compares the energy efficiencies of several applications. O_3 generation was listed as a benchmark reaction because of its long-standing implementation on the industrial scale. The highest O_3 generation yields are 550 g-O_3/kWh (O_2 sources). The plasma-catalysis of water (H_2 source) and air (N_2 source) seems to be less efficient for NH_3 production [264]. The average energy consumption of NH_3 synthesis is approximately 36.6 GJ/ton-NH_3 [244], which corresponds to 107.1 g-NH_3/kWh. HC reforming for H_2 production constitutes approximately 80 % of the energy consumption, so the net energy yield of the HB process is estimated to be about 500 g-NH_3/kWh. Considering the low adaptivity of the HB process for downsizing, the benchmark energy yield for 10 ton-NH_3/d is in the range of 150–200 g-NH_3/kWh. The plasma-catalysis yield (25–30 g-NH_3/kWh) must

Table 3 Energy efficiency of NH_3 formation using plasma or plasma-catalysis

Reaction	Energy yield	Remarks	Ref
$N_2 + 3H_2 \rightarrow 2NH_3$	500 g-NH_3/kWh	HB process (Net yield excluding reforming process)	–
Air $\rightarrow HNO_3$	67 g-HNO_3/kWh	BE process (arc plasma)	252
CH_4 + Air $\rightarrow NH_3$	1.0 g-NH_3/kWh	Microplasma (without catalyst)	258
$N_2 + 3H_2 \rightarrow 2NH_3$	0.06 g-NH_3/kWh	Ru, Pt, Ni, Fe loaded membrane reactor	262
$N_2 + H_2O \rightarrow 2NH_3$	0.2 g-NH_3/kWh (estimated)	Plasma-catalysis (Fe/Alumina) NH_3 20 ppm (N_2:H_2O = 37.5:5.1)	264
$N_2 + 3H_2 \rightarrow 2NH_3$	25–30 g-NH_3/kWh	Plasma-catalysis (Ru-Mg/Alumina) (N_2:H_2 = 80:20)	This study
$O + O_2 + M \rightarrow O_3 + M$	300–500 g-O_3/kWh	Benchmark reaction (O_2-fed ozonizer)	–

therefore be increased at least 10 fold more for practical use. It is worth mentioning that the current value was obtained at a single-pass under atmospheric pressure, and can be further increased with increased pressure.

Summary

In this review, the current status of plasma-catalysis has been discussed. We have also emphasized the need for a multidisciplinary approach to this field, because many of the plasma-catalysis interactions have a bilateral nature. Despite the numerous experimental reports on the synergy effect in plasma-catalysis, the development of a fundamental understanding of the surface reactions is still in the early stages. The accumulation of related experimental data facilitate tuning of plasma-catalysis in target reactions. The followings is a brief summary of prominent open questions on the possible interactions between plasma and catalysts.

- Can an electric field promote surface diffusion and/or surface reactions?
- Can EHD flow promote mass transfer from the gas-phase to the surface?
- What are the surface reactive species fixed under plasma application? How and where are they fixed on the surface?
- Will in situ measurement of surface reactions or temporal surface changes be possible?

Acknowledgments The authors wish to acknowledge the support from the Grant-in-aid for Scientific Research (C) (26400539), and from the Council for Science, Technology and Innovation (CSTI), Cross-ministerial Strategic Innovation Promotion Program (SIP), "Energy Carrier" (Funding agency: JST). One of authors (H.H. Kim) thank Dr. Sylvain Touchard, Dr. Arlette Vega-Gonzalez, and Prof. Xavier Duten of Universite Paris 13, LSPM (CNRS) for their help in preparing the manuscript.

References

1. Mizuno A, Clements JS, Davis RH (1986) IEEE Trans Ind Appl 22(3):516–522
2. Clements JS, Mizuno A, Finney WC, Davis RH (1989) IEEE Trans. Ind Appl 25(1):62–69
3. Mizuno A, Yamazaki Y, Ito H, Yoshida H (1992) IEEE Trans Ind Appl 28(3):535–540
4. Nunez CM, Ramsey GH, Ponder WH, Abbott JH, Hamel LE, Kariher PH (1993) J. Air Waste Manag Assoc 42:242–247

5. US EPA. Air pollution and the clean air act. Available online: http://www.epa.gov/air/caa/
6. Penetrante BM, Schultheis SE (1993) Non-thermal plasma techniques for pollution control: part a: overview, fundamentals and supporting technologies. Springer-Verlag, New York, p 397
7. Penetrante BM, Schultheis SE (1993) Non-thermal plasma techniques for pollution control: part b: electron beam and electrical discharge processing. Springer-Verlag, New York, p 397
8. Dinelli G, Civitano L, Rea M (1990) IEEE Trans Ind Appl 26(3):535–541
9. Masuda S, Nakao K (1990) IEEE Trans Ind Appl 26(3):374–383
10. Ohkubo T, Kanazawa S, Nomoto Y, Chang JS, Adachi T (1994) IEEE Trans Ind Appl 30(4):856–861
11. Yan W, Ninghui W, Yimin Z, Yanbin Z (1998) J Electrostat 44:11–16
12. Amirov RH, Chae JO, Dessiaterik YN, Filimonova EA, Zhelezniak MB (1998) Jpn J Appl Phys 37:3521–3529
13. Park JY, Tomicic I, Round GF, Chang JS (1999) J Phys D Appl Phys 32:1006–1011
14. Mok YS, Nam IS (1999) IEEE Trans Plasma Sci 27(4):1188–1196
15. Masuda S, Hosokawa S, Tu X, Tsutsumi M, Ohtani T, Tsukahara T, Matsuda N (1993) IEEE Trans Ind Appl 29(4):774–780
16. Yamamoto T, Ramanathan K, Lawless PL, Ensor DS, Newsome JR, Plaks N, Ramsey GH (1992) IEEE Trans Ind Appl 28(3):528–534
17. Evans D, Rosocha LA, Anderson GA, Coogan JJ, Kushner MJ (1993) J Appl Phys 74(9):5378–5386
18. Chang MB, Lee CC (1995) Environ Sci Technol 29:181–186
19. Yamamoto T, Chang JS, Berezin AA, Kohno H, Honda S, Shibuya A (1996) J Adv Oxid Technol 1(1):67–78
20. Oda T, Yamashita R, Haga I, Takahashi T, Masuda S (1996) IEEE Trans Ind Appl 32(1):118–124
21. Tonkyn RG, Barlow SE, Orlando TM (1996) J Appl Phys 80(9):4877–4886
22. Hsiao MC, Penetrante BM, Merritt BT, Vogtlin GE, Wallman PH (1997) J Adv Oxid Technol 2(2):306–311
23. Futamura S, Zhang AH, Yamamoto T (1997) J Electrostat 42:51–62
24. Falkenstein Z (1999) J Appl Phys 85(1):525–529
25. Cal MP, Schluep M (2001) Environ Prog 20(3):151–156
26. Yang C, Beltran M, Kravets Z, Yamamoto T (1998) Environ Prog 17(3):183–189
27. Chang MB, Lee HM, Wu F, Lai CR (2004) J. Air Waste Manag Assoc 54:941–949
28. Higashi M, Uchida S, Suzuki N, Fujii K (1992) IEEE Trans Plasma Sci 20(1):1–12
29. Mizuno A, Shimizu K, Matsuoka T, Furuta S (1995) IEEE Trans Ind Appl 31(6):1463–1468
30. Chakrabarti A, Mizuno A, Shimizu K, Matsuoka T, Furuta S (1995) IEEE Trans Ind Appl 31(3):500–506
31. Wei ZS, Li HQ, He JC, Ye QH, Huang QR, Luo YW (2013) Bioresour Technol 146(1):451–456
32. Paur HR, Baumann W, Lindner W, Matzing H (1992) Radiat Phys Chem 40(4):273–278
33. Roland U, Holzer F, Kopinke F-D (2002) Catal Today 73:315–323
34. Holzer F, Roland U, Kopinke F-D (2002) Appl Catal B Environ 38:163–181
35. Roland U, Holzer F, Kopinke FD (2005) Appl Catal B Environ 58:217–226
36. Ogata A, Yamanouchi K, Mizuno K, Kushiyama S, Yamamoto T (1999) IEEE Trans Ind Appl 35(6):1289–1295
37. Kim HH, Takashima K, Katsura S, Mizuno A (2001) J Phys D Appl Phys 34:604–613
38. Broer S, Hammer T (2000) Appl Catal B Environ 28:101–111
39. Miessner H, Francke K-P, Rudolph R, Hammer T (2002) Catal Today 75:325–330
40. Mok YS, Koh DJ, Kim KT, Nam IS (2003) Ind Eng Chem Res 42:2960–2967
41. Kusic H, Koprivanac N, Locke BR (2005) J Hazard Mater B125:190–200
42. Wang H, Li J, Quan X, Wu Y, Li G, Wang F (2007) J Hazard Mater 141:336–343
43. Bubnov AG, Burova EY, Grinevich VI, Rybkin VV, Kim JK, Choi HS (2006) Plasma Chem Plasma Process 26(1):19–30
44. Liu CJ, Zou J, Yu K, Cheng D, Han Y, Zhan J, Ratanatawanate C, Jang BWL (2006) Pure Appl Chem 78(6):1227–1238
45. Liu CJ, Zhao Y, Li Y, Zhang DS, Chang Z, BU WH (2013) ACS Sustain Chem Eng 2(1):3–13
46. Ho KY, Yeung KL (2006) J Catal 242(1):131–141
47. Ray AB, Anderegg FO (1921) J Am Chem Soc 43(5):967–978
48. Anderegg FO (1923) Trans Am Electrochem Soc 44:203–214
49. Anderegg FO, Herr WN (1925) J Am Chem Soc 47(10):2429–2431
50. Gallon H, Kim HH, Tu X, Whitehead JC (2011) IEEE Trans Plasma Sci 39(11):2176–2177
51. Newsome PT (1926) J Am Chem Soc 48:2035–2045
52. Boelter KJ, Davidson JH (1997) Aerosol Sci Technol 27:689–708
53. Yehia A, Mizuno A (2008) Int J Plasma Environ Sci Technol 2(1):44–49

54. Maltsev AN, Eremin EN, Belova VM (1971) Russ J Phys Chem 45(7):1042–1043
55. Maltsev AN, Eremin EN, Belova VM (1974) Russ J Phys Chem 48(8):1229–1231
56. Maltsev AN, Eremin EN, Belova VM (1974) Russ J Phys Chem 48(8):1256–1257
57. Belova VM, Eremin EN, Maltsev AN (1978) Russ J Phys Chem 52(7):968–970
58. Eremin EN, Belova VM, Maltsev AN (1978) Russ J Phys Chem 52(7):970–972
59. Chen X, Rozak J, Lin JC, Suib SL, Hayashi Y, Matsumoto H (2001) Appl Catal A Gen 219:25–31
60. Thomas CL, Egloff G, Morrell JC (1941) Chem Rev 28:1–70
61. Henis JM (1976) Nitrogen oxide decomposition process. USA. U.S. Patent 3,983,021
62. Schmidt-Szalowski K, Borucka A (1989) Plasma Chem Plasma Process 9(2):235–255
63. Schmidt-Szalowski K, Jodzis S, Krawczyk K, Mlotek M, Gorska A (2006) Curr Top Catal 5:39–68
64. Morinaga K, Suzuki M (1962) Bull Chem Soc Jpn 35(2):249–307
65. Tanaka M, Ogawa S, Wada N, Yoshiyasu H, Yagi S (2005) IEEJ Trans FM 125:817–822 **(in Japanese)**
66. Toyofuku M, Ohtsu Y, Fujita H (2004) Jpn J Appl Phys 43(7A):4368–4372
67. Bo Z, Yu K, Lu G, Mao S, Chen J, Fan FG (2010) Environ Sci Technol 44:6337–6342
68. Liang B, Ogino A, Nagatsu M (2010) J Phys D Appl Phys 43(27):275202
69. Yurevich V, Maxim K, Malashin V, Moshkunov SI, Shershunova EA, Yamschikov VA (2014) IEEE Trans Plasma Sci 42(10):3314–3320
70. Osawa N, Yoshioka Y (2012) IEEE Trans Plasma Sci 40(1):2–8
71. Jodzis S (2003) Ozone Sci Eng 25:63–72
72. Kim H-H, Teramoto Y, Negishi N, Ogata A (2015) Catal Today 256:13–22. doi:10.1016/j.cattod.2015.04.009
73. Jia Z, Vega-Gonzalez A, Amar MB, Hassouni K, Tieng S, Touchard S, Kanaev A, Duten X (2013) Catal Today 208:82–89
74. Huang H, Ye D, Guan X (2008) Catal Today 139:43–48
75. Fan X, Zhu T, Sun Y, Yan X (2011) J Hazard Mater 196:380–385
76. Ogata A, Saito K, Kim HH, Sugasawa M, Aritani H, Einaga H (2010) Plasma Chem Plasma Process 30:33–42
77. Chang CL, Lin TS (2005) Plasma Chem Plasma Process 25(4):387–401
78. Durme JV, Dewulf J, Sysmans W, Leys C, Langenhove HV (2007) Appl Catal B Environ 74:161–169
79. Wallis AE, Whitehead JC, Zhang K (2007) Catal Lett 113(1–2):29–33
80. Huu TP, Gil S, Costa PD, Giroir-Fendler A, Khacef A (2015) Catal Today 257:86–92. doi:10.1016/j.cattod.2015.03.001
81. Wang Q, Yan BH, Jin Y, Cheng Y (2009) Energy Fuel 23:4196–4201
82. Kim HH, Tsubota S, Daté M, Ogata A, Futamura S (2007) Appl Catal A Gen 329:93–98
83. Kim HH, Sugasawa M, Hirata H, Teramoto Y, Kosuge K, Negishi N, Ogata A (2013) Plasma Chem Plasma Process 33(6):1083–1098
84. Yoshida H, Marui Z, Aoyama M, Sugiura J, Mizuno A (1989) J Inst Electrostat Jpn 13(5):425–430
85. Hübner M, Guaitella O, Rousseau A, Röpcke J (2013) J Appl Phys 114(3):033301
86. Harling AM, Glover DJ, Whitehead JC, Zhang K (2008) Environ Sci Technol 42(12):4546–4550
87. Sivachandiran L, Thevenet F, Rousseau A (2015) Chem Eng J 270:327–335
88. Sivachandiran L, Thevenet F, Rousseau A (2014) Chem Eng J 246:184–195
89. Kim HH, Oh SM, Ogata A, Futamura S (2005) J Adv Oxid Technol 8(2):226–233
90. Kim HH, Ogata A, Futamura S (2008) Appl Catal B Environ 79:356–367
91. Fan HY, Shi CS, Li XS, Zhao DX, Xu Y, Zhu AM (2009) J Phys D Appl Phys 42(22):225105
92. Mok YS, Kim DH (2011) Curr Appl Phys 11:S58–S62
93. Kang WS, Lee DH, Lee JO, Hur M, Song YH (2013) Environ Sci Technol 47:11358–11362
94. Kogelschatz U (2003) Plasma Chem Plasma Process 23(1):1–46
95. Harling AM, Kim HH, Futamura S, Whitehead JC (2007) J Phys Chem C 111(13):5090–5095
96. Kuzumoto M, Ogawa S, Yagi S (1989) J Phys D Appl Phys 22:1835–1839
97. Yasui K, Kuzumoto M, Ogawa S, Tanaka M, Yagi S (1989) IEEE J Quantum Electron 25(4):836–840
98. Sano T, Negishi N, Sakai E, Matsuzawa S (2006) J Mole Catal A Chem 245:235–241
99. Ochiai T, Nakata K, Murakami T, Morito Y, Hosokawa S, Fusishima A (2011) Electrochemistry 79(10):838–841
100. Kim HH, Oh SM, Ogata A, Futamura S (2005) Appl Catal B Environ 56(3):213–220
101. Huang HB, Ye DQ, Fu ML, Feng FD (2007) Plasma Chem Plasma Process 27:577–588
102. Rousseau A, Guaitella O, Gatilova L, Thevenet F, Guillard C, Ropcke J, Stancu GD (2005) Appl Phys Lett 87:221501
103. Khastgir SR (1952) J Chem Phys 20:1052–1053
104. Bhide VG, Bhiday MR, Asolkar GV (1952) Nature 169:542–543

105. Falkenstein Z (1997) J Appl Phys 81(11):7159–7162
106. Falkenstein Z (1997) J Appl Phys 81(9):5975–5979
107. Gosho Y (1982) J Phys D Appl Phys 15:1217–1225
108. Nygaard KJ (1965) Rev Sci Instrum 36(9):1320–1323
109. Baricos J, Dupuy J, Peyrous R, Schreiber G (1978) J Phys D Appl Phys 11:L187–L190
110. Kim C, Park D, Noh KC, Hwang J (2010) J Electrostat 68:36–41
111. Tajalli H, Lamb DW, Woolsey GA (1989) J Phys D Appl Phys 22:1497–1503
112. Moreau E, Touchard G (2008) J Electrostat 66:39–44
113. Kanazawa S, Shuto Y, Sato N, Ohkubo T, Nomoto Y, Mizeraczyk J, Chang JS (2003) IEEE Trans Ind Appl 39(2):333–339
114. Jogan K, Mizuno A, Yamamoto T, Chang JS (1993) IEEE Trans Ind Appl 29(5):876–881
115. Ogata A, Shintani N, Mizuno K, Kushiyama S, Yamamoto T (1999) IEEE Trans Ind Appl 35(4):753–759
116. Wang D, Matsumoto T, Namihira T, Akiyama H (2010) J Adv Oxid Technol 13(1):71–78
117. Stratton BC, Knight R, Mikkelsen DR, Blutke A, Vavruska J (1999) Plasma Chem Plasma Process 19(2):191–216
118. Huang L, Zhang XW, Chen L, Lei LC (2011) Plasma Chem Plasma Process 31:67–77
119. Lee DH, Song YH, Kim KT, Lee JO (2013) Plasma Chem Plasma Process 33:647–661
120. Yang Y (2002) Ind Eng Chem Res 41(24):5918–5926
121. Herron JA, Tonelli S, Mavrikakis M (2013) Surf Sci 614:64–74
122. Burrow PD (1973) J Chem Phys 59(9):4922–4931
123. Thomas JM, Kaufman F (1985) J Chem Phys 83(6):2900–2903
124. Nozaki T, Muto N, Kado S, Okazaki K (2004) Catal Today 89(1–2):57–65
125. Nozaki T, Muto N, Kadio S, Okazaki K (2004) Catal Today 89(1–2):67–74
126. Kim HH, Ogata A, Schiorlin M, Marotta E, Paradisi C (2011) Catal Lett 141(2):277–282
127. Guaitella O, Lazzaroni C, Marinov D, Rousseau A (2010) Appl Phys Lett 97:011502
128. Guaitella O, Hubner M, Welzel S, Marinov D, Ropcke J, Rousseau A (2010) Plasma Sources Sci Technol 19:045206
129. Marinov D, Guaitella O, Booth JP, Rousseau A (2013) J Phys D Appl Phys 46(3):032001
130. Teramoto Y, Kim HH, Ogata A, Negishi N (2013) Catal Lett 143:1374–1378
131. Oh SM, Kim HH, Einaga H, Ogata A, Futamura S, Park DW (2006) Thin Solid Films 506–507:418–422
132. Rideal EK, Kunz K (1920) J Phys Chem 24:379–392
133. Li W, Gibbs GV, Oyama ST (1998) J Am Chem Soc 120:9041–9046
134. Teramoto Y, Kim HH, Negishi N, Ogata A (2015) Catalysts 5:838–850
135. Yamamoto T, Tanioka G, Okubo M, Kuroki T (2007) J Electrostat 65:221–227
136. Yoshida K, Okubo M, Yamamoto T (2007) Appl Phys Lett 90:131501
137. Yamamoto T, Okubo M, Kuroki T (2000) Trans Inst Fluid-Flow Mach 107:111–120
138. Okubo M, Tanioka G, Kuroki T, Yamamoto T (2002) IEEE Trans Ind Appl 38(5):1196–1203
139. Somorjai GA (1992) Catal Lett 12(1–3):17–34
140. Motret O, Hibert C, Pellerin S, Pouvesle JM (2000) J Phys D Appl Phys 33:1493–1498
141. Ono R, Nifuku M, Fujiwara S, Horiguchi S (2005) J Appl Phys 97(12):123307
142. Ono R, Teramoto Y, Oda T (2010) Plasma Sources Sci Technol 19(1):015009
143. Komuro A, Ono R, Oda T (2010) Plasma Sources Sci Technol 19(5):055004
144. Teramoto Y, Ono R (2014) J Appl Phys 116(7):073302
145. Ishikawa K, Sumi N, Kono A, Horibe H, Takeda K, Kondo H, Sekine M, Hori M (2011) J Phys Chem Lett 2(11):1278–1281
146. Ishikawa K, Mizuno H, Tanaka H, Tamiya K, Hashizume H, Ohta T, Ito M, Iseki S, Takeda K, Kondo H, Sekine M, Hori M (2012) Appl Phys Lett 101(1):013704
147. Su H, Hou Y, Houk RS, Schrader GL, Yeung ES (2001) Anal Chem 73:4434–4440
148. Su H, Yeung ES (2000) J Am Chem Soc 122(30):7422–7423
149. Teramoto Y, Kim HH, Ogata A, Negishi N (2014) J Appl Phys 115(13):133302
150. Aydil ES, Gottscho RA, Chabal YJ (1994) Pure Appl Chem 66(6):1381–1388
151. Aissa KA, Semmar N, Achour A, Simon Q, Petit A, Camus J, Boulmer-Leborgne C, Djouadi MA (2014) J Phys D Appl Phys 47(35):355303
152. Tu X, Gallon HJ, Twigg MV, Gorry PA, Whitehead JC (2011) J Phys D Appl Phys 44(27):274007
153. Lee H, Song HK, Min BR (2006) Catal Lett 35(6):646–647
154. Jwa E, Lee SB, Lee HW, Mok YS (2013) Fuel Process Technol 108:89–93
155. Haruta M, Kobayashi T, Sano H, Yamada N (1987) Chem Lett 2:405–408
156. Haruta M, Yamada N, Kobayashi T, Iijima S (1989) J Catal 115:301–309

157. Haruta M, Tsubota S, Kobayashi T, Kageyama H, Genet MH (1993) J Catal 144:175–192
158. Fan HY, Shi CA, Li XS, Zhang S, Liu JL, Zhu AM (2012) Appl Catal B Environ 119:49–55
159. Li WX, Stampfl C, Scheffler M (2002) Phys Rev B 65(7):075407
160. Shi H, Stampfl C (2007) Phys Rev B 76(7):075327
161. Bray JM, Schneider WF (2011) Langmuir 27:8177–8186
162. Ray NK, Anderson AB (1982) Surf Sci 119:35–45
163. Turner M, Glovko VB, Vaughan OPH, Abdulkin P, Berenguer-Murcia A, Tikhov MS, Johnson BFG, Lambert RM (2008) Nature 454:981–984
164. Kim HH, Kim JH, Ogata A (2009) J Phys D Appl Phys 42:135210
165. Kim HH, Teramoto Y, Sano T, Negishi N, Ogata A (2015) Appl Catal B Environ 166–167:9–17
166. Kim HH, Ogata A (2012) Int J Plasma Environ Sci Technol 6(1):43–48
167. Teramoto Y, Kim HH, Ogata A, Negishi N (2014) IEEE Trans Plasma Sci 42(10):2850–2851
168. Deshlahra P, Schneider WF, Bernstein GH, Wolf EE (2011) J Am Chem Soc 133:16459–16467
169. Lee J, Sorescu DC, Deng X (2011) J Am Chem Soc 133:10066–10069
170. Kim HH, Ogata A, Futamura S (2005) J Phys D Appl Phys 38(8):1292–1300
171. Argyle MD, Bartholomew CH (2015) Catalysts 5:145–269
172. Kameshima S, Tamura K, Ishibashi Y, Nozaki T (2015) Catal Today 256:67–75. doi:10.1016/j.cattod.2015.05.011
173. Liu X, Mou CY, Lee S, Li Y, Secrest J, Jang BWL (2012) J Catal 285:152–159
174. Zou JJ, He H, Cui L, Du HY (2007) Int J Hydrogen Energy 32:1762–1770
175. Chen HL, Lee HM, Chen SH, Chang MB, Yu SJ, Li SN (2009) Environ Sci Technol 43:2216–2227
176. Durme JV, Dewulf J, Leys C, Langenhove HV (2008) Appl Catal B Environ 78:324–333
177. Sultana S, Vandenbroucke AM, Leys C, Geyter ND, Morent R (2015) Catalysts 5:718–746
178. Chen HL, Lee HM, Chen SH, Chang MB (2008) Ind Eng Chem Res 47(7):2122–2130
179. Thevenet F, Sivachandiran L, Guaitella O, Barakat C, Rousseau A (2014) J Phys D Appl Phys 47(22):224011
180. Whitehead JC (2010) Pure Appl Chem 82(6):1329–1336
181. Baeva M, Dogan A, Ehlbeck J, Pott A, Uhlenbusch J (1999) Plasma Chem Plasma Process 19(4):445–466
182. Yan K, Kanazawa S, Ohkubo T, Nomoto Y (1999) Plasma Chem Plasma Process 19(3):421–443
183. Masuda S, Hosokawa S, Tu X, Sakakibara K, Kitoh S, Sakai S (1993) IEEE Trans Ind Appl 29(4):781–786
184. Tokunaga O, Nishimura K, Machi S, Washino M (1978) Int J Appl Radiat Isotopes 29:81–85
185. Zhao G-B, Garikipati SVBJ, Hu X, Argyle MD, Radosz M (2005) AIChE J 51(6):1800–1812
186. Einaga H, Ogata A (2009) J Hazard Mater 164:1236–1241
187. Dang X, Huang J, Cao L, Zhou Y (2013) Catal Commun 40:116–119
188. Zhao DZ, Li XS, Shi C, Fan HY, Zhu AM (2011) Chem Eng Sci 66:3922–3929
189. Kim HH (2004) Plasma Process Polym 1(2):91–110
190. Mizuno A (2013) Catal Today 211:2–8
191. Penetrante BM, Brusasco RM, Merritt BT, Vogtlin GE (1999) Pure Appl Chem 71(10):1829–1835
192. Djéga-Mariadassou G, Baudin F, Khacef A, Costa PD (2012) NOx abatement by plasma catalysis. In: Lukes P, Parvulescu VI, Magureanu M (eds) Plasma chemistry and catalysis in gases and liquids. Wiley-VCH, USA, pp 89–129
193. Hammer T, Broer S (1998) Society of automotive engineers: paper no. 982428
194. Hammer T, Broer S (1999) Society of automotive engineers:paper no. 1999-1901-3633
195. Nelo SK, Leskela KM, Sohlo JJK (1997) Chem Eng Technol 20:40–42
196. Fujishima H, Kuroki T, Ito T, Otsuka K, Yamamoto T, Yoshida K, Okubo M (2010) IEEE Trans Ind Appl 46(5):1707–1714
197. Mok YS (2006) Chem Eng J 118:63–67
198. Mizuno A, Shimizu K, Chakrabarti A, Dascalescu L, Furuta S (1995) IEEE Trans Ind Appl 31(5):957–963
199. Koebel M, Elsener M, Madia G (2001) Ind Eng Chem Res 40(1):52–59
200. Stevenson SA, Vartuli JC (2002) J Catal 208:100–105
201. Mok YS, Dors M, Mizerazcyk J (2004) IEEE Trans Plasma Sci 32(2):799–807
202. Kato A, Matsuda S (1998) Nihon Kagakukaishi (6):406–411
203. Iwamoto M (1990) Chem. Lett. 1967–1970
204. Iwamoto M, Yahiro H (1994) Catal Today 22:5–18
205. Yoon S, Panov AG, Tonkyn RG, Ebeling AC, Barlow SE, Balmer ML (2002) Catal Today 72:243–250
206. Tonkyn RG, Barlow SE, Hoard JW (2003) Appl Catal B Environ 40:207–217
207. Lee JO, Song YH, Cha MS, Kim SJ (2007) Ind Eng Chem Res 46(17):5570–5575

208. Kim HH, Takashima K, Katsura S, Mizuno A (1999) In: *low temperature scr process using pulsed corona discharge*, annual meeting of IEJ, Chiba, Japan, 1999; IEJ: Chiba, Japan, p.219–222
209. Lee DH, Lee JO, Kim KT, Kim E, Han HS (2011) Int J Hydrogen Energy 36:11718–11726
210. Costa CN, Savva PG, Fierro JLG, Efstathiou AM (2007) Appl Catal B Environ 75:147–156
211. Liu Z, Li J, Woo SI (2012) Energy Environ Sci 5:8799–8814
212. Lee DH, Lee JO, Kim KT, Song YH, Kim E, Han HS (2012) Int J Hydrogen Energy 37:3225–3233
213. Yoshida K, Kuwahara T, Kuroki T, Okubo M (2012) J Hazard Mater 231–232:18–25
214. Okubo M, Inoue M, Kuroki T, Yamamoto T (2005) IEEE Trans Ind Appl 41(4):891–899
215. Wang H, Yu Q, Liu T, Xiao L, Zheng X (2012) RSC Adv 2:5094–5097
216. Leray A, Guy A, Makarov M, Lombaert K, Cormier JM, Khacef A (2013) Top Catal 56:222–226
217. Nozaki T, Okazaki K (2013) Catal Today 211:29–38
218. Tao X, Bai M, Li X, Long H, Shang S, Yin Y, Dai X (2011) Prog. Energy Combust Sci 37(2):113–124
219. Chao Y, Lee HM, Chen SH, Chang MB (2009) Int J Hydrogen Energy 34:6271–6279
220. Hong RF, Lai MP, Chang YP, Yur JP, Hsieh SF (2009) Int J Hydrogen Energy 34:6280–6289
221. Chen HL, Lee HM, Chen SH, Chao Y, Chang MB (2008) Appl Catal B Environ 85:1–9
222. Zhang X, Dai B, Zhua A, Gonga W, Liu C (2002) Catal Today 72:223–227
223. Marafee A, Liu C, Xu G, Mallinson R, Lobban L (1997) Ind Eng Chem Res 36:632–637
224. Rico VJ, Hueso JL, Cotrino J, Gonzalez-Elipe AR (2010) J Phys Chem A 114(11):4009–4016
225. Kasinathan P, Park S, Choi WC, Hwang YK, Chang JS, Park YK (2014) Plasma Chem Plasma Process 34:1330–1370
226. Li Y, Xu G-H, Liu C-J, Eliasson B, Xue B-Z (2001) Energy Fuel 15:299–302
227. Zhang K, Eliasson B, Kogelschatz U (2002) Ind Eng Chem Res 41:1462–1468
228. Pornmai K, Jindanin A, Sekiguchi H, Chavadej S (2012) Plasma Chem Plasma Process 32:723–742
229. Kabashima H, Einaga H, Futamura S (2001) Chem. Lett. 1314–1315
230. Koo IG, Lee WM (2007) Electrochem Commun 9:2325–2329
231. Rico VJ, Hueso JL, Cotrino J, Gallardo V, Sarmiento B, Brey JJ, Gonzalez-Elipe AR (2009) Chem Commun 41:6192–6194. doi:10.1039/B909488a
232. Du CM, Mo JM, Li HX (2015) Chem Rev 115:1503–1542
233. Horng RF, Huang HH, Lai MP, Wen CS, Chiu WC (2008) Int J Hydrogen Energy 33:3719–3727
234. Sobacchia MG, Savelieva AV, Fridmana AA, Kennedya LA, Ahmedb S, Krauseb T (2002) Int J Hydrogen Energy 27:635–642
235. Okumoto M, Rajanikanth BS, Katsura S, Mizuno A (1998) IEEE Trans Ind Appl 34(5):940–944
236. Eliasson B, Kogelschatz U, Xue B, Zhou L (1998) Ind Eng Chem Res 37:3350–3357
237. Mok YS, Kang HC, Koh DJ, Shin DN, Baik JH (2010) J Korean Phys Soc 57(3):451–457
238. Kumamoto A, Iseki H, Ono R, oda T (2011) J Phys. Conference series 301:012039
239. Ono R, Oda T (2008) Combust Flame 152:69–79
240. Klerke A, Christensen CH, Norskov JK, Vegge T (2008) J Mater Chem 18(20):2285–2310
241. Choudhary TV, Sivadinarayana C, Goodman DW (2001) Catal Lett 72(3–4):197–201
242. Kroch E (1945) J. Inst Pet 31:213–223
243. Reiter A (2009) Combustion and emissions characteristics of a compression-ignition engine using dual ammoniadiesel fuel. Iowa State University, Country
244. (IEA) I.E.A. (2007) *Tracking industrial energy efficiency and CO_2 emission,* International Energy Agency (IEA)
245. Kadowaki Y, Aika K (1996) J Catal 161:178–185
246. You Z, Inazu K, Aika K, Baba T (2007) J Catal 251:321–331
247. Kitano M, Inoue Y, Yamazaki Y, Hayashi F, Kanbara S, Matsuishi S, Yokoyama T, Kim SW, Hara M, Hosono H (2012) Nat Chem 4:934–940
248. Licht S, Cui B, Wang B, Li FF, Lau J, Liu S (2014) Science 345(6197):637–640
249. Lan R, Tao S (2013) RSC Adv 3:8016–18021
250. Marnellos G, Stoukides M (1998) Science 282:98–100
251. Lan R, Irving JTS, Tao S (2013) Sci Rep 3:1145
252. Egeland A, Leer E (1986) IEEE Trans Plasma Sci 14(6):666–677
253. Birkeland K. Manufacture of concentrated nitric acid. US. 1,23,662, 1917
254. Hessel V, Anastasopoulou A, Wang Q, Kolb G, Lang J (2013) Catal Today 211:9–28
255. Anastasopoulou A, Wang Q, Hessel V, Lang J (2014) Processes 2:694–710
256. Patil BS, Wang Q, Hessel V, Lang J (2015) Catal Today
257. Wendt GL, Snyder JE (1928) J Am Chem Soc 50:1288–1292
258. Bai M, Zhang Z, Bai M, Bai X, Gao H (2008) J Air Waste Manag Assoc 58:1616–1621
259. Bai M, Bai X, Zhang Z, Bai M (2000) Plasma Chem Plasma Process 20:511–520

260. Yeh GC. Method of producing ammonia including contacting an electrostatically charged catalyst with nitrogen and hydrogen. USA. 3,344,052, 26 Sept 1967
261. Sugiyama K, Akazawa K, Oshima M, Miura H, Matsuda T, Nomura O (1986) Plasma Chem Plasma Process 6(2):179–193
262. Mizushima T, Matsumoto K, Ohkita H, Kakuta N (2007) Plasma Chem Plasma Process 27(1):1–11
263. Brewer AK, Miller RR (1931) J Am Chem Soc 53(8):2968–2978
264. Gieshoff J, Lang J (2002) Process for the plasma-catalytic production of ammonia. US. 6,471,932 B1